BUDAPEST UNIVERSITY OF TECHNOLOGY AND ECONOMICS
FACULTY OF MECHANICAL ENGINEERING
DEPARTMENT OF MATERIALS SCIENCE AND ENGINEERING

TUDOMÁNYOS DIÁKKÖRI KONFERENCIA

Luka Radulovic
(Mechanical Engineering Programme BSc, 5. Term)

Zinc foams manufactured via sintering

Consultant(s):
Dr. Wiener Csilla

Budapest, 2023

DECLARATIONS

Declaration of acceptance

This thesis fully complies with the requirements of the Faculty of Mechanical Engineering of the Budapest University of Technology and Economics for the Scientific Student Conference in terms of content and form, as well as with the objectives. I consider this thesis to be suitable for public evaluation and public presentation.

Date of submission: 5.11.2023.

……

Supervisor

Declaration on independent work

I, the undersigned, Luka Radulovic (IVPST0), a student of the Budapest University of Technology and Economics, being aware of my criminal and disciplinary responsibility, hereby declare and certify with my own signature that I have prepared this thesis on my own without any unauthorized assistance and that I have used only the sources provided. All passages taken verbatim or in the same sense but paraphrased from other sources have been clearly indicated by citing the source in accordance with the applicable regulations.

Budapest, 05.11.2023.

……

student

Table of Contents

1. Summary

Metal foams are cellular materials comprising solid metallic phase with a substantial volume of gas-filled pores. The pores can be either interconnected, known as open-cell foams, or isolated by solid matter, called closed-cell foams. These materials find diverse applications; closed cell metal foams are used in energy absorption and structural support system, while open-cell foams are suitable for applications such as filtration systems and heat exchangers.

Typically, the solid material for metal foams is aluminium; however, metal foams made of materials like copper, titanium, and magnesium are also manufactured and utilized. There are certain metals, including magnesium, iron, and zinc, which are classified as biodegradable materials and they all hold potential for the production of temporary implants. Metal foams possess cellular structures similar to bones, making zinc foams particularly appealing as candidates for bone implants. As zinc foams degrades, it can be gradually replaced by bone tissue during the healing process, thus, the removal surgery can be avoided rendering them highly promising for orthopaedic applications.

Production methods for zinc foams are still being developed. They are primarily powder metallurgical method, where compaction of the zinc powder with space holder particles is followed by sintering. In our research, we have adopted a recently discovered method known as chemical sintering, aiming to lower production costs and duration. We investigated the effect of various production parameters, and we have successfully fabricated zinc foams with promising mechanical properties. The extent to which chemical sintering can reduce the duration of subsequent hot sintering while still achieving satisfactory mechanical properties was also investigated. Furthermore, we explore potential adjustments in production parameters to further reduce the required hot sintering time

2. Introduction

2.1. Properties and applications

The term metal foam refers to cellular materials comprised of solid metallic phase containing significant quantity of gas-filled cavities, referred to as pores. This type of structure strongly resembles natural biological structures, such as marine sponges, timber, and notably bone. This structure allows metal foams to have impressive stiffness and energy absorption abilities while having a relatively light weight.[(1), (2)]

Due to very significant differences in the structure of foams, mechanical properties, as well as applications, a clear distinction can be made between open-cell (Figure 1a [(3)]) and closed-cell metal foams (Figure 1b [(4)]). Open-cell foams are characterised by interconnected pores, resulting in higher porosity (volume fraction of pores), thus making them particularly suited for applications related to heat exchangers and filtration[(5), (6), (7)]. The increased porosity results in lower overall strength. Conversely, pores in closed-cell foams are separated by solid material.

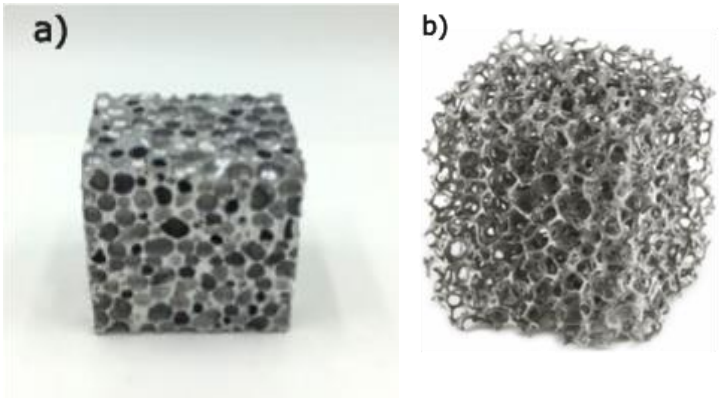

Figure 1. Structure of a closed-cell aluminium metal foam (a) and an open cell metal foam (b)

One of the most outstanding properties of metal foams is their specific energy absorption capacity. This unique trait arises due to their cellular structure, which allows them to absorb a substantial amount of mechanical energy while deforming without exceeding a certain stress level. In practice, this causes them to plastically deform up to a high strain while experiencing close to constant stress (Figure 2 [(8)]). This characteristic makes closed-cell foams especially well-suited for utilization in energy-absorption systems, such as vehicular bumpers [(1), (9)].

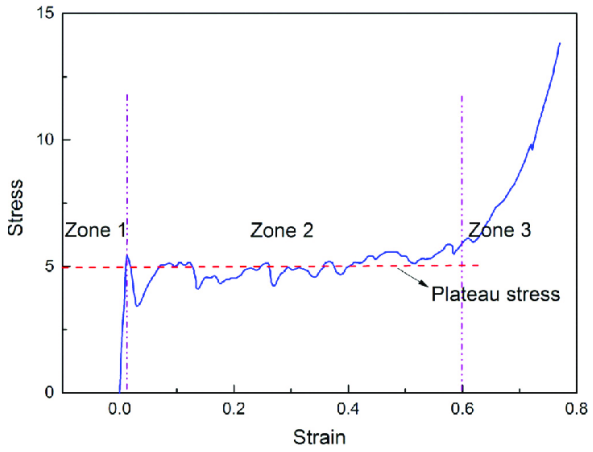

Figure 2. typical stress-strain diagram for metal foams with a marked plateau region

Most properties of metal foams scale with the density in according to the following formula [(10)]:

$$\frac{P_{foam}}{P_{solid}} = A\left(\frac{\rho_{foam}}{\rho_{solid}}\right)^{n}$$

Here P_{foam} and P_{solid} represent a chosen property of the foam and the bulk material that the foam is made of, respectively; ρ_{foam} and ρ_{solid} are the density of the foam and bulk material, respectively and A are constants that may depend on multiple factors like the manufacturing method, the structure, shape of the cells, deformation mechanism etc. and n is constant that depends on the mode of deformation.

Increasing the strength of the solid material naturally increases the strength of the metal foam as well, it is thus possible to apply hardening methods such as heat treatment (if the bulk material is heat treatable), alloying etc. also on metal foams [(11), (12)].

Their impressive specific stiffness in combination with their outstanding energy absorption capabilities at relatively low weight leads to the utilization of metal foams in a variety of fields ranging from construction, architecture (Figure 3a [(3)]) and kinetic energy absorbers such as car bumpers, all the way to filtration, thermodynamical applications (Figure 3b [(13)]) and even certain applications in the medical field (Figure 3c [(1)]).

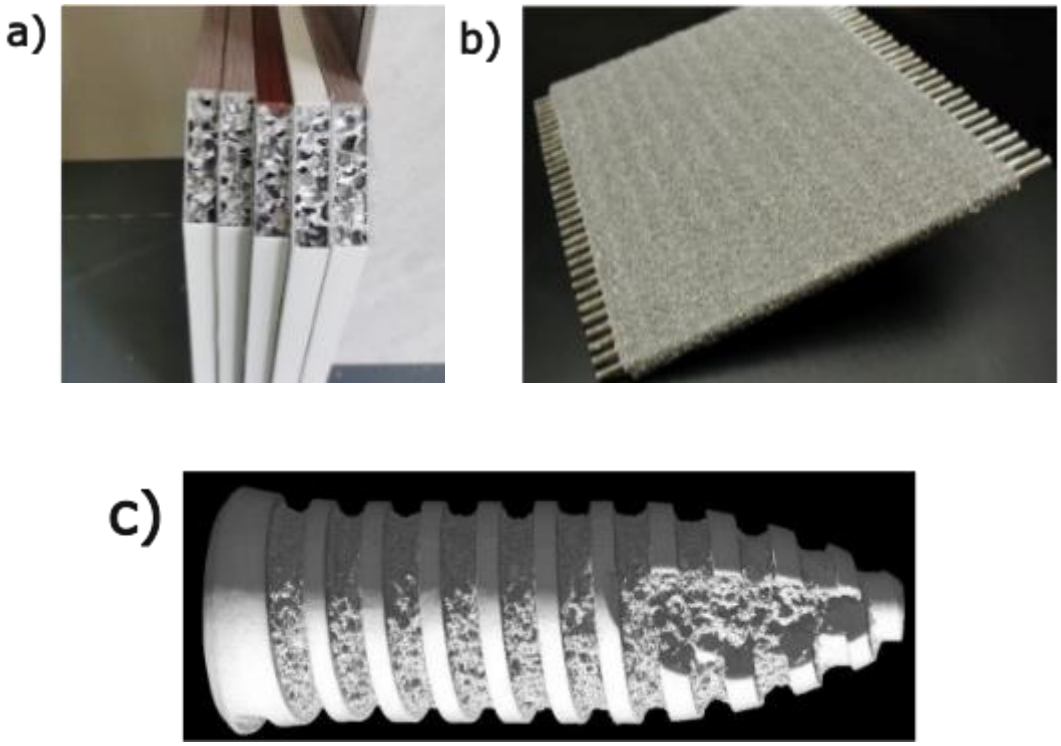

Figure 3. metal foam used as an insulator (a), a new type of metal foam heat exchanged (b) and a metal foam dental implant (c)

2.2. Production methods

There are multiple manufacturing methods to produce metal foams and the applied method depends on the desired application. The most common manufacturing methods are the following [(1), (2), (14), (15)]:

- Gas injection foaming

One of the most wide-spread methods to make aluminium and aluminium alloy foams is the gas injection foaming method. As the name suggests, using special impellers or nozzles gas, usually oxygen, nitrogen or argon is injected into the molten metal [(16)] as seen on Figure 4 [(14)]. The formed bubbles must be stabilized, therefore, ceramic particles such as silicon-carbide are first mixed into the material and the melt's viscosity is also increased (e.g., by adding Ca). Typical porosities are ranging about from about 6vol.% to 20vol.%.

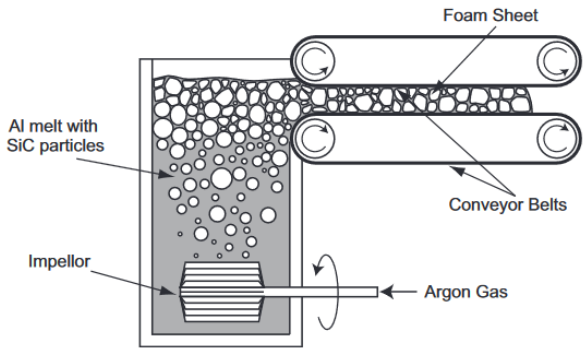

Figure 4. schematic representation of the gas injection foaming manufacturing process

- Blowing agent foaming

Similar to the Gas Injection method, the viscosity of the melt needs to be increased before foaming which is usually achieved by adding calcium oxide[(17)] as seen on Figure 5 [(14)]. Once the desired viscosity has been achieved, titanium hydride (TiH_2) is added to the melt which releases hydrogen gas into the hot viscous liquid, creating porosities inside it.

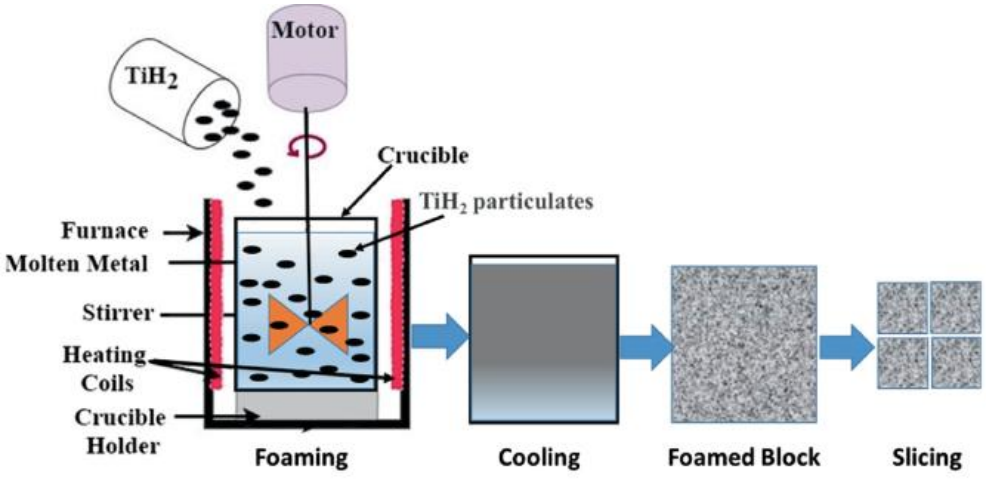

Figure 5 schematic representation of the blowing agent manufacturing process

- Powder compact foaming using blowing agent

Metal foams can also be made from metal powders [(18)]. The first step of this method is to mix the metal powder or a powder blend with a blowing agent after which it is compacted. The next step is to heat up the workpiece to temperatures near the matrix material's melting temperature. The foaming agent, which is homogeneously distributed, will start decomposing and expanding resulting in a foamed metal as seen in Figure 6 [(14)].

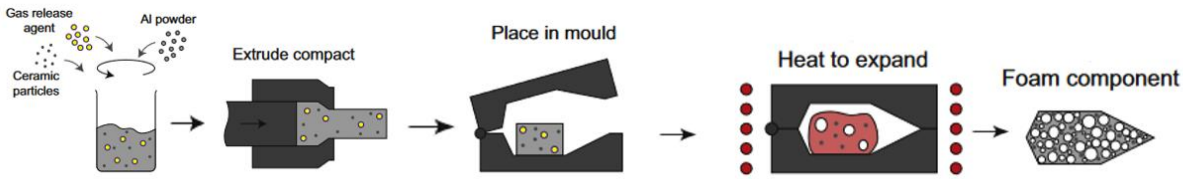

Figure 6 schematic representation of the powder compact foaming manufacturing process

- Space holder method

This method uses different types of soluble granules, usually water soluble, to occupy the space of the pores inside the material [(19),]. A structure made of these granules is infiltrated with molten metal, which is going to be the matrix. Once the structure is solidified the soluble particles are leached leaving us with an open-celled foam as seen in Figure 7 [(14)].

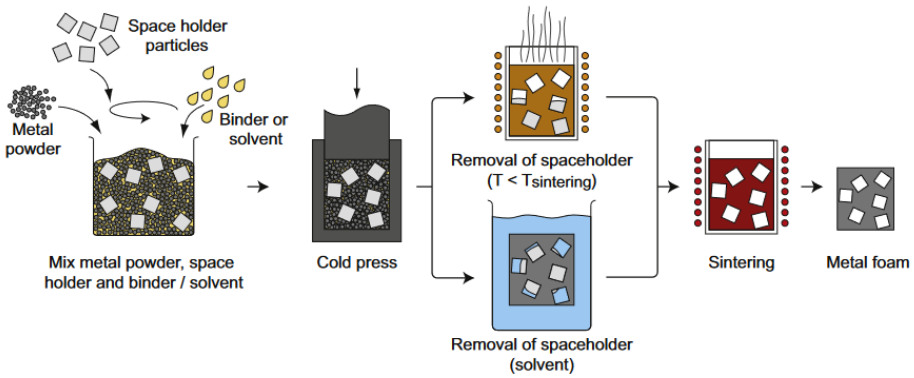

Figure 7 schematic representation of the space holder manufacturing process

There are many, altogether different processes, such as polymer sponge-based foams [(20)], ingot foaming, eutectic-solidified foams [(14)] etc. that were not discussed to avoid digressing too much. As it can be seen the possible methods, just like their variations are numerous, and combinations of different methods are naturally also possible. Notably, for our research purposes, a combination of the space holder and the powder compact methods was used in consideration of our goals.

Production methods of metal foams, and metal foams themselves, are still being very actively researched due to their many possible applications and customizable properties. Among these applications, alternative implants stand out and such implants are already used [(21)]. By adjusting the relative density of the metal foam, similar mechanical properties to bone can be produced, which makes them desirable for medical applications. Structural and mechanical requirements aside, the material itself needs to be compatible with the human body. Up till now only biocompatible metals are one possible solution for this because they don't have a negative impact on the body, but a possibly better alternative would be biodegradable materials [(22), (23)]. Their quality of being degraded by biological processes could allow for the self-removal of implants with time. This could eliminate the need for an implant removal surgery after a bone prosthetic has been implanted because the body dispose of it with time.

2.3. Objectives

Manufacturing methods for zinc foams according to the literature are very limited [(11), (24), (25)]. Few methods exist for producing zinc foams: the classic powder metallurgical method as discussed previously, through electrochemical decomposition of zinc on copper, and through the powder metallurgical method in combination with the space holder method.

Very recently, a new technique has been developed for producing printable inks for electrical applications using zinc nanoparticles [(26)]. This method uses acid to sinter the zinc particles to each other through a chemical reaction between the acid and the oxide layer of the zinc particles. This method is called chemical or cold sintering depending on the literature. Due to

the nature of the application, the mechanical properties of the sintered zinc were not investigated.

Our research will investigate the potential of this method in the production of zinc foams in a more efficient and economical way. One very significant difference between the previous chemical sintering methods and ours is that our will be carried out at much higher pressures. This was done because certain literature showed that the higher the compaction pressure the higher the mechanical strength of metal foams in the case of the powder metallurgy method combined with the space holder method [(24)].

Our previous work has already established that it is indeed possible to create zinc foams with this method, but the compressive properties were not satisfactory. The objective of our current work is to investigate how to further improve the compressive properties of the chemically sintered zinc foams as well as to investigate the possible optimisation of hot sintering using our previous results.

3. Review of literature

3.1. Mechanical properties

Extensive research has already been done on metal foams, their mechanical properties as well as the effect that production methodology and parameters have on the foams.

As mentioned previously, metal foams have good specific energy absorption properties due to their peculiar stress-strain curve. The stress-strain curve of metal foams is divided into 3 parts:

1. Quasi-linear stage – Here the stress increases almost linearly with the strain, but local plastic deformation still occurs due to the very strong geometric inhomogeneity.
2. Plateau region – In this region the stress in some cases remains very close to a constant value as the strain increases [(27)]. In some other cases, depending on the metal material's properties, it shows wavy characteristics [(11)], however, increasing stress in this region was also measured (deformation of open-cell aluminum foam). During the plateau region the cells collapse; the exact mechanism of cell collapse depends on the material. Once all of the cells have collapsed the last stage commences.
3. Densification – As the cells have collapsed, upon further compression these already collapsed cells are densified decreasing the remnant porosity of the foam. At the end of the densification stage, the foam behaves similar to the bulk material during compression [(27)].

For mechanical applications the following data is the most important: the stiffness of the foam, the plateau stress and the end of the plateau region, the energy absorption and energy absorption efficiency. These terms have been standardized according to ISO 13314:2011 [(28)] as follows:

Plateau stress – The arithmetic mean stress measured in the interval between 20% and 30% or 20% and 40% compressive strain.

Plateau end – The strain at which the stress is higher than 130% of the plateau stress.

Energy absorption – The area under the stress-strain curve up to 50% strain or up to the plateau end strain.

Energy absorption efficiency – Energy absorption divided by the product of the maximum stress within the strain range and the magnitude of the strain range.

The stiffness of the foam can be considered as the slope of the engineering stress-strain curve in the quasi-linear stage.

A stress-strain diagram with the relevant values marked can be seen on Figure 8 [(28)].

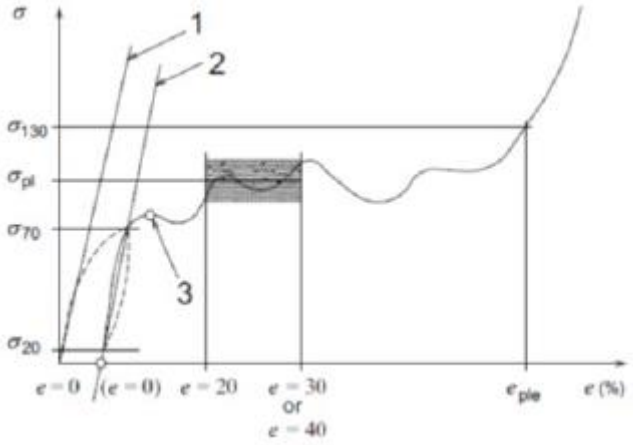

Figure 8 A simplified stress strain diagram of a metal foam where plateau stress is calculated in the region between 20% and 30% deformation with the end of the plateau marked as σ_{130}

3.2 Production and mechanical properties of Zn foams

Research on the production of zinc foams in general is still very novel, only a few reported on some results of Zn foam manufacturing, and only two of them investigated pure zinc foam production. Two manufacturing methods have been reported about the production of pure zinc foam in the literature so far. One of them using the powder compaction method together with space holder particles resulting in an open-cell foam [(24)], while the other is a powder metallurgical method using a blowing agent to produce a closed-cell foam [(25)].

Xiaodong et al. have successfully manufactured a Copper-Zinc metal foam through the electrodeposition of zinc [(29)]. Steel meshes as well as carbon-based substrates were investigated as alternative substrates, but Copper foam was found to be the most suitable for the electrodeposition of zinc. The purpose of these substrates was to make it possible to use zinc as an anode material, having applications in electronic components. Only the electrical and chemical properties of these foams were investigated.

Sadighikia et al. have successfully manufactured open-cell zinc foams with porosities in the range of 74%-92% using the space holder technique [(25)], one such sample can be seen on Figure 9. In their research, they coated carbide particles with the zinc metal powder and compacted it at high pressure before leaching out the carbide particles and then sintered it. They found that the optimum properties were achieved with a compacting pressure of 300MPa and sintering temperature of 410˚C for 2 hours.

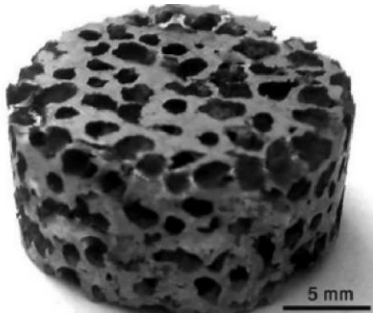

Figure 9. Image of a zinc metal foam produced using the space holder technique

At compaction pressures below 200MPa the green strength was too low, and the samples could not remain intact after leaching, while at pressures above 400MPa the carbide granules started to deform and break apart, resulting in some pores being cracked or crushed. The compression tests results can be seen on Figure 10a/b.

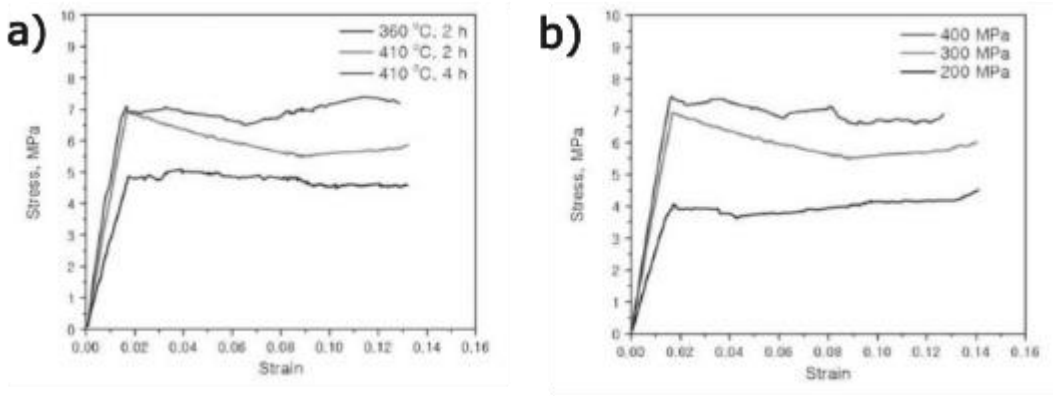

Figure 10. Comparison of stress-strain curves of specimens sintered at different temperatures (a) and compacted at different durations (b)

Kovacik et al. successfully manufactured pure Zn and Zn alloy metal foams through the powder metallurgical method using a blowing agent [(25)]. The low melting temperature of zinc posed a significant challenge due to being below the optimum temperature for the hydrogen gas release from the TiH_2. The possibility of using alternative blowing agents such as MgH_2 was investigated but it resulted in unsatisfactory foaming. The final solution was to increase the amount of foaming agent to compensate for the reduced foaming and the temperature was further increased beyond the melting point of zinc. The higher temperature reduced the viscosity of the foam resulted in porosities up to 92% and in a density gradient along the vertical axis because of gravity which can be seen on Figure 11.

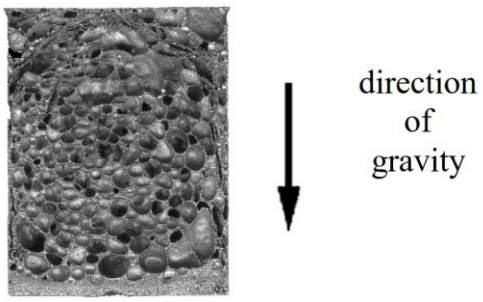

Figure 11. The structure of a zinc foam made using the powder metallurgical method with a visible gradient in pore distribution along the direction of gravity

During compression tests a drop in stress was observed at the beginning of the compression which can be seen on Figure 12. The reason for this was the collapse of the weakest structures in the less dense regions of the foam.

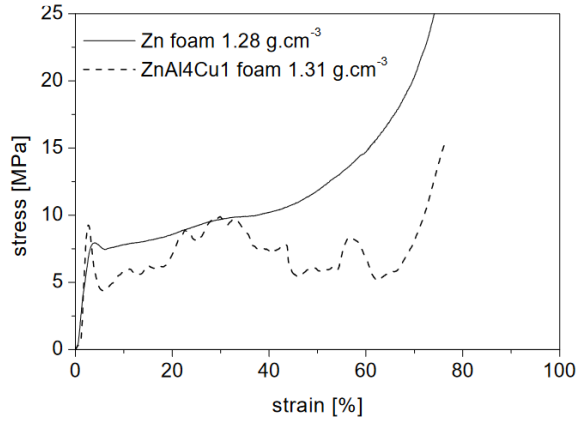

Figure 12. Stress-strain diagram of the compressed zinc and zinc alloy foams with visible drop at the end of the quasi-elastic region

Banhart et. al. [(11)] also manufactured zinc alloy metal foam containing 4 wt.% Cu using the powder metallurgical method. One research goal was to investigate the possibilities of heat treating the aluminium foams they made during this research. The other goal was to investigate the effects the outer skin as well as the pore orientation had on the compression strength of the samples. Compressing the samples under different orientations showed differences in compressive strength for the same production parameters, which can be seen on Figure 13a/b. This knowledge could be used to further tailor the properties of metal foams to their applications.

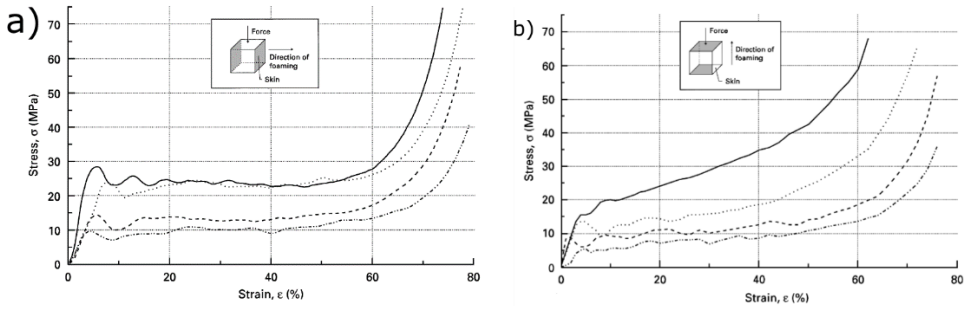

Figure 13. The stress-strain diagram of samples compressed perpendicular to the direction of foaming (a) and parallel to the direction of foaming (b)

J. Banhart et al., in a different article, also made pure zinc metal foam using the powder metallurgical method [(30)]. Pure zinc powder was mixed with 0.3 wt.% ZrH_2, which was used as a blowing agent was hot pressed at 350 ˚C for 30 min. For foaming a furnace was preheated at 440 ˚C. The main goal of this research was to investigate the pore formation process, therefore the foaming was stopped at different foaming times and analysed through ultra small-angle neutron scattering. The highest porosity achieved was 20% and the mechanical properties were left uninvestigated as it was not in the scope of the research.

3.3 Chemical sintering of solid metals

The technique of chemical sintering is still A very novel powder metallurgical method and, therefore, the amount of literature on the topic is very limited, with no mention of chemically sintered foams having been found. There is only one research paper where chemicals were used to create a high temperature environment to sinter an indium, bismuth and tin alloy at a temperature of 200 ˚C [(31)]. This process relies on a complicated combination of chemical reactions to reach sintering temperatures and is not applicable to materials that require higher sintering temperatures.

The chemical sintering that we investigated is significantly different. Majee et al. discovered that Zn nanoparticles can be sintered at almost room temperatures by their technique of chemical sintering, which they used to make an ink for printing. The printing process was as follows:

1. Printing the ink mixture containing zinc nanoparticles in solvent
2. Drying the films to evaporate the solvent (60 ˚C for a few minutes is sufficient)
3. Overprinting the curing ink over the dried zinc films
4. Drying the final films

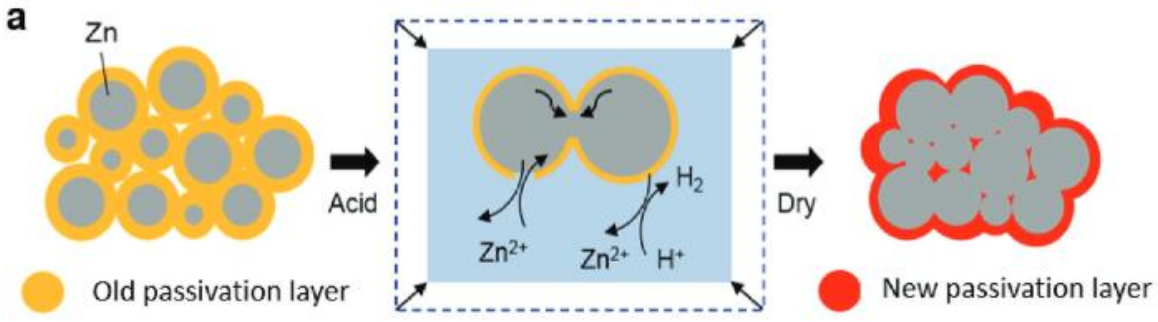

Figure 14. A schematic representation of the chemical reaction driving the chemical sintering of zinc particles

Essentially, the chemical sintering occurs due to an interaction between the Zn powder and the aqueous solution of acetic acid (H_2O:CH_3COOH=10:1) where a self-exchange of Zn and Zn^{2+} occurs at the Zn/H_2O interface under the acidic conditions, shown in a more simplified form on Figure 14.

This technique was used only for the manufacturing of electric components, so modifications had to be made to make metal foams.

4. Experimental and results

This section will discuss both the production and results of the chemically sintered foams. Because there is no existing research in chemically sintered foams, the production parameters had to be adjusted and the effects of the production parameters on the mechanical performance had to be investigated repeatedly throughout the research and modified adequately. For the purpose of easier reasoning, the results of each step are presented together with its description.

The compression tests were carried out on an Instron 5965 at a constant cross-head speed of 0.6 mm/min.

4.1 Experimental

4.1.1 Preliminary research

The initial research which was conducted focused on exploring the feasibility of cold sintering and the main production parameters that could affect the mechanical properties of the final product.

Preliminary testing was conducted in cooperation with Professor Thalmaier, an expert in powder metallurgy, who also investigated chemical sintering. At the beginning of the research, two specimens were made using NaCl of different sizes as a placeholder. One specimen was made with NaCl grains with a diameter between 0.8 mm and 1 mm, while the second one had NaCl grains with a diameter between 0.5 mm and 0.8 mm. Both specimens had a 50:50 wt.% NaCl-Zn ratio and 0.5 ml of ethanol was added as an adhesive. The shape of the zinc powder particles was spherical. The specimens were placed into a die and 0.5 ml of 100% acetic acid was added to each side of the specimen before it was compacted at 30 kN for 5 minutes with a Tira Test 2100 mechanical testing machine. The samples were afterwards grinded to remove the outer skin and leached for 24 hours under running tap water before being analysed under a scanning electron microscope (SEM). The results were that the samples tended to crumble after prolonged contact with water and traces of NaCl were detected in the foam. The conclusion was that a different space holder was necessary, and urea was selected due to its water solubility, low evaporation temperature and sufficient strength.

In the next test, a 40:60 vol% Zn-Urea mixture was made with an average granule diameter of 2.8 mm. Ethanol was again used as an adhesive (0.5ml) and 0.5ml of acid to each side of the specimen before compacting them at 30 kN for 5 minutes. Specimens with a greater height were more prone to breaking apart due to improper sintering. SEM analysis showed that the sintering was partly successful, motivating further research. The issue of lacking structural integrity persisted thus the adhesive was changed to polyvinyl acetate (PVA).

Compression tests were not conducted on the first few samples as they were produced mainly to investigate the feasibility of chemical sintering with the help of an SEM. Compression tests were carried out on latter few samples of this series.

Afterwards, Professor Thalmaier designed a die for compaction. Until the equipment was machined, we used cut iron pipe segments as a die for compaction. Different production parameters were tested but it was very difficult to make satisfactory specimens. One of the main observations was that from the different volume ratio mixtures that were made, that a 50:50 vol.% Zn-urea mixture was the most successful. Only a single specimen with 40:60

vol.% Zn-urea didn't crumble during leaching, and not a single 60:40 vol.% Zn-Urea specimen managed to retain structural integrity. Even though they did not immediately crumble, the samples that retained structural integrity could still be easily broken into pieces by hand, indicating insufficient sintering. During the compaction, the highest pressure allowed by the pipes was 250MPa, which dropped down to 125MPa by the end of the compaction. The conclusion was that high pressure is essential for proper sintering and that a 50:50vol.% had a larger likelihood of being successfully sintered which proved to be true later. A notable observation was that the sample made with the cut steel pieces had ellipsoidal pores due to the lateral deformation of the material of the pipe, which might be useful for producing anisotropic foams.

The last observations made during the preliminary test were during the production of more 50:50 vol.% specimens. The specimens were made taking the previous observations into account, in addition to being compacted at 500MPa for 5 minutes in the newly designed die set. Acetic acid was added while mixing the powder and urea (1.5ml) and to both sides of the specimen before compaction. Both water leaching and evaporation at elevated temperatures were used to remove the urea from the foam. The final specimen had a visibly inhomogeneous pore distribution in its structure. It is important to note that in all these cases there were significant difficulties in the removal of the samples, and we suspected that the amount of liquid in the mixture may be a partial cause of this. To minimize the amount of the liquid used, the mixture was created only right before compaction, reducing the amount of the evaporated acid. A total of 5 drops of both acid and PVA solution were dropped with a pipette into the powder mixture. The zinc powder in this series as well as all future samples was made from Zn powder with irregular particle shape. This modification was made since chemical sintering is also an area-dependent process, making better sintering possible with the increased contact surface area of irregular particles.

Compression tests showed that the samples could reach a maximum compression strength of up to 14 MPa, but after reaching this maximum the samples started crumbling due to cracks, causing a drop in strength. This resulted in stress-strain curves that were missing a well-defined plateau region, which is characteristic for metal foams. The stress strain curve of one of the samples used can be seen on Figure 15.

The figure shows that the specimen deformed linearly up to a pressure of 17MPa, after which it started cracking and crumbling resulting in a steep drop in stress which is why the figure lacks the plateau region characteristic for metal foams.

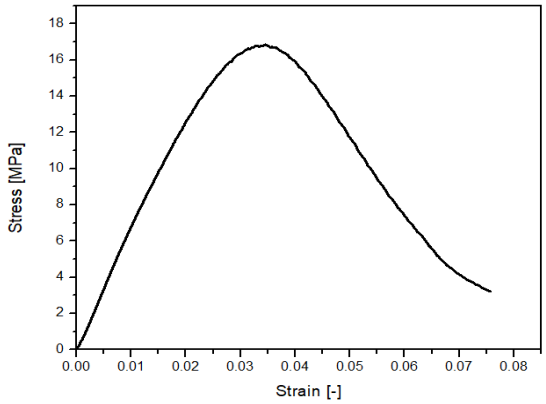

Figure 15 stress-strain diagram from the compression test of one of the samples from the initial research

One specimen was also hot sintered at 420 ˚C for 4 h in vacuum to set a reference, the stress-strain diagram can be seen on Figure 16. The initial quasi-linear stage was similar to the one of the cold sintered sample, reaching an initial peak at 22 MPa before the plateau region was achieved. The shape of the plateau region indicates reduced efficency in energy absoprtion, but it is still very similar in shape to Banhart's measurements in Figure 13b indicating that the sintering was a success and is a usable refernce.

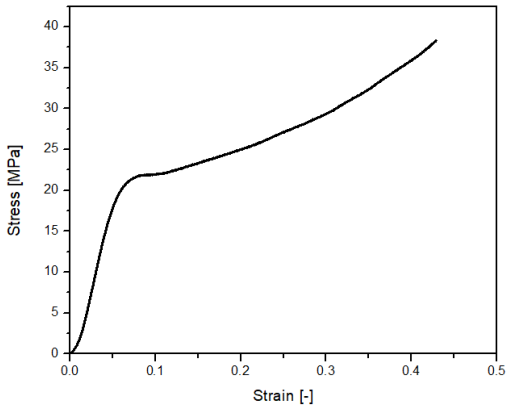

Figure 16. Stress-strain diagram from the compression test of the hot sintered sample

4.1.2 Effects of different production parameters

After it was established that the cold sintering was possible, further research was done to determine how to improve the mechanical properties of the metal foams, primarily strength and specific energy absorption. The effects of the following production parameters were investigated: (i) mixing technology, (ii) acid content, (iii) method of adding acid, (iv) compaction pressure, (v) multistage compaction, (vi) drying, (vii) adhesive modifications and (viii) sintering time. The effect of some of the parameters were only investigated visually, that is the integrity of the sample was checked after leaching. If the sample could maintain its integrity during the whole procedure, the compressive properties such as compressive strength and plateau stress were determined. The effects of the investigated parameters were the following.

i. **Mixing technology**

The mixing technology used up to this point consisted of thoroughly stirring the mixture with a glass stirring rod inside a plastic container not much larger than the final specimen. Professor Thalmaier suggested that we should try mixing the urea and zinc inside a tumble mixer and provided us with his own specimens made this way. Due to a lack of equipment, efforts were made to create a similar equipment from a container. The powder mixture was mixed by rotating the container for 2 hours at $50s^{-1}$. The final product was visually similar Professor Thalmaier's, but neither his nor ours managed to be leached successful. The conclusion was that during tumble mixing the urea granules were not properly coated even after increasing the amount of adhesive by six times to compensate for the losses due to adhering to the wall.

ii. **Acid content**

As stated previously, the amount of liquid used was reduced to make the removal of the samples easier. The effect of the amount of acid on the production method was also investigated. The tests were made with two times and five times the usual acid content (10 and 20/25 drops from the pipette compared to the usual 5 drops). No notable difference was observed in the samples made this way. The reason behind the similar quality was the very high pressures pushing the acid out through the gaps between the punches and the die, resulting in effectively a similar amount of acid acting during the chemical sintering at high pressure.

iii. **Addition of acid**

In our previous findings, we established that acid should be added only at the latest possible moment to minimizing the evaporation. Previously, this was done by adding the acid to the mixture before compaction and stirring it before placing it into the die. This was further improved by placing the mixture into the die in 3 increments without mixing the acid into it and then 1-2 drops of acid were added on the top of the mixture. This resulted in slightly better final products with a higher sintering success rate, but no notable strength differences.

iv. **Compaction pressure**

Previously a 300 MPa compaction pressure was used. This was done in consideration of both the die's strength as well as the strength of urea granules used as a placeholder. After testing, both the die and urea managed to withstand up to 700 MPa without problems. At this pressure, the final specimen was compacted even more, resulting in overall more successful sintering and higher leaching success rates.

v. **Multistage compaction**

Due to the internal stress distribution, the middle of the specimen experiences the smallest pressure during compaction, leading to worse sintering quality and structural inhomogeneity and making the success rate of samples with a higher height/diameter ratio less successful. We attempted compaction in multiple stages, i.e. compacting a fraction of the mixture at ~200 MPa before adding the next portion and repeating this procedure until the mixture was used up. The goal was to initiate slight sintering on each portion first and compact the entire structure more evenly. The result was that the portions could not be connected after pre-compacting them even at these relatively low pressures, turning each portion into a separate smaller specimen that easily detaches from the complete structure without any damage. This might be a possible method to create multiple samples at once in a taller die, but the dimensions of our die did not allow us to test this possibility.

vi. **Drying**

The primary purpose of the adhesive was to evenly coat the urea particles with the Zn powder to help with homogenous distribution of the particles, and the secondary purpose was to help the specimen retain structural integrity after leaching out the urea particles. The listed drying time for PVA to take effect is between 30 minutes and an hour which still was not satisfactory. After increasing the drying time to 24 hours, a noticeable reduction was observed in the number of unsuccessful leaching attempts.

vii. Adhesive modification

During the preliminary testing, a PVA solution was found to be an effective adhesive to help the samples retain structural integrity after leaching in water. One drawback of the mixture was the high water content, which resulted in a paste-like mixture with lower viscosity after mixing the adhesive into the metal powder and urea mixture, making the manufacturing more difficult. It resulted in a highly heterogeneous distribution of urea particles and possibly making leaching more difficult to execute. Substituting the water with acetic acid was attempted with the goal of the acid evaporating during the sintering and drying process. The result was successful with no decrease in strength, and the samples could be easily leached out.

All of the investigated factor up to this point helped with the production, increasing leaching success rate and improving production efficiency overall. At this point, samples with a compressive strength of 7MPa could be reliably produced. Although it was less than the desired strength, it is still sufficient for electronic applications. A typical stress strain curve of samples at this point can be seen in Figure 17 The main challenge at this point was the unsatisfactory stress strain curve, lacking the characteristic plateau shape due to the brittle behaviour of the specimens.

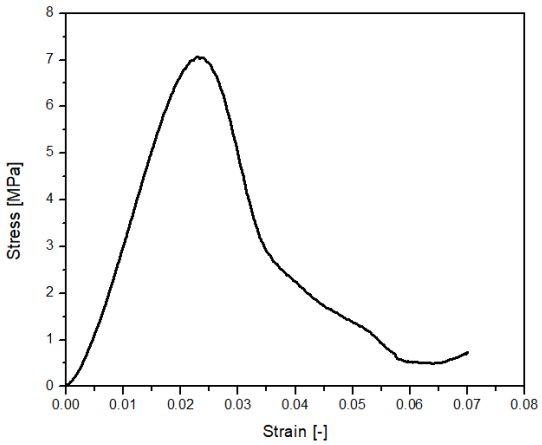

Figure 17 typical stress-strain diagram of specimens that were being produced at this time

Another challenge was the reduced compressive strength of the samples compared to the initially manufactured ones (compare Figure 15 and Figure 17). After a few months, the compressive strength of the samples produced by the same way with the same manufacturing parameters started to decrease. The cause of this phenomenon was investigated later along with similar issues.

viii. Time for compaction

Although chemical sintering is different from hot sintering, which is a time dependent process, the chemical reaction driving chemical sintering is likewise a time dependent process. For this reason, specimens were kept under the same final compaction pressure (700 MPa) for different amounts of time. The investigated compaction times were 10 min, 30 min, 1h and 2h. There was no notable difference in the strength and the compressive behaviour of the foams keeping after keeping them under pressure at or below of 1 hour, but there were significant differences observed at the 2 hour compacting durations. The

two specimens that were kept under pressure for 2 hours and later compressed exhibited a significantly better energy absorption during compression testing, in the form of a more pronounced plateau like the hot sintered sample.

Figure 18a and Figure 18b show that the behaviour of the samples differed significantly from the previous ones. There is a stress drop after the end of the quasi-linear stage, but the samples did not directly crumble after reaching the peak stress and absorbs a higher amount of energy during compression. This indicated a step in the right direction, but the reduced strength of these samples was unexpected and, therefore, we investigated it later.

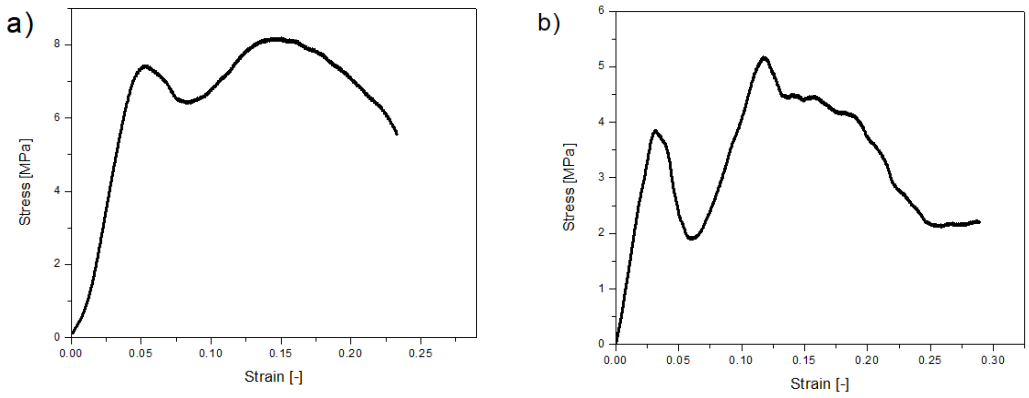

Figure 18. Stress strain diagram of the first (a) and second (b) samples made with a 2h compaction time showing a more defined plateau region

4.1.3 Comparison to hot sintering

The final experiments set carried out investigated the possibility of reducing the time required for hot sintering by chemically sintering the specimen first.

Six specimens were chemically sintered at 700 MPa for 5 minutes with 6 drops of acetic acid together with 6 drops of a PVA:acid 25:75vol.% ratio mixture in a Zn:urea 50:50vol.% ratio, the final weights and heights between 4.5 g and 5 g and 11.5 mm and 12.5 mm, respectively. Three more samples were made without any chemical sintering, with a PVA:water solution at a 25:75vol.% ratio, using 6 drops of the PVA solution. The compaction pressure and time were the same as beforehand (700MPa, 10 min.) and the final dimensions and weights of these samples were similar to the previous ones.

After chemical sintering, the 6 specimens were also hot sintered at 410˚C inside a small container connected to an argon tank with a volume flow rate of 1l/min to avoid oxidization. In this environment 3 samples were sintered for 30 min and the remaining 3 for 1 h. As a reference, the three specimens compacted with only 6 drops of adhesive were sintered for 2 hours under the same conditions. (The experiment was originally designed for the vacuum furnace built by Professor Blücher, where the temperature could have been controlled very precisely, but due to an unfortunate accident the furnace couldn't be used in the last 3 months.)

The first source of error was the furnace, which was designed for temperatures up to 1200˚C, making it less precise at lower temperatures. The other source of error was the cooling effect of the argon which was supplied to the container, causing an uncertain difference in temperature inside the container compared to the temperature displayed by the thermometer.

Due to the sintering quality being strongly influenced by the sintering temperature, small deviation in this range can cause very significant differences in sintering quality, making these errors a considerable factor of the sintering quality. However, the hot sintering settings were the same in each case, so the comparison of the additionally hot sintered samples is possible.

The final compression results can be seen on Figure 19a/b/c. Not only was there a lack of any kind of improvement in the sintering quality in the previously chemically sintered samples, even the samples that were completely hot sintered showed very low compression strength. This was a huge discrepancy with our previous results which warranted an immediate investigation of the issue.

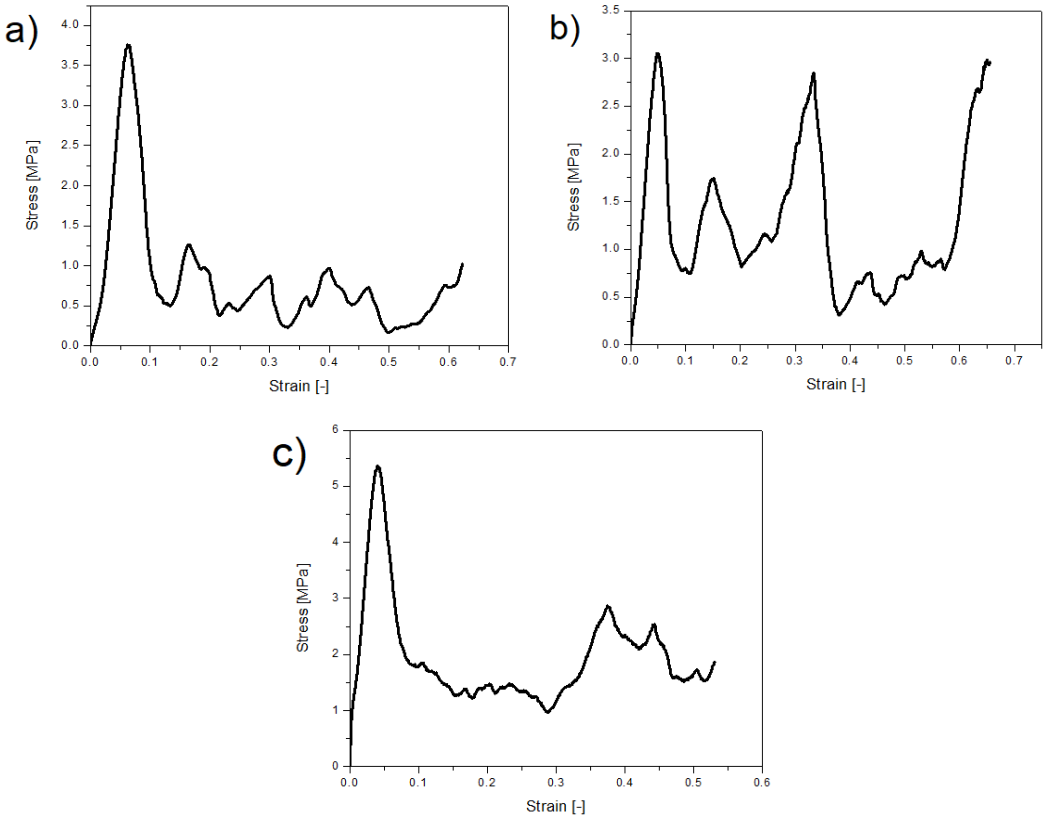

Figure 19. Stress strain diagram of samples that were first chemically sintered and the hot sintered for 30 min (a) and 1h (b) respectively together with the purely hot sintered sample (c) showing reduced strengths

4.1.4 General compression data

Because of the similar typical stress-strain curves (that is, they have a quasi-linear part, and after the peak stress the stress drops to a very low value, which is followed by a serrated stress-strain curve with low stress values), the samples can be compared by their compressive strengths. The scatter in strength is very significant as can be seen on Figure 20a/b and the porosity and the height of the sample seem to be the determining factors. According to Table 1 with increasing porosity the strength of the material is decreasing, while with decreasing height the strength of the material also decreases. The samples with porosities above 60% were mostly manufactured in new attempts to sinter higher porosity samples, but the results were not satisfactory, and the attempts were stopped. On the graphs it can be more clearly seen that for samples with a height/diameter ratio close to or below 1 and porosities above

60% the strength decreases significantly. Table 1 contains the exact data from the compression tests.

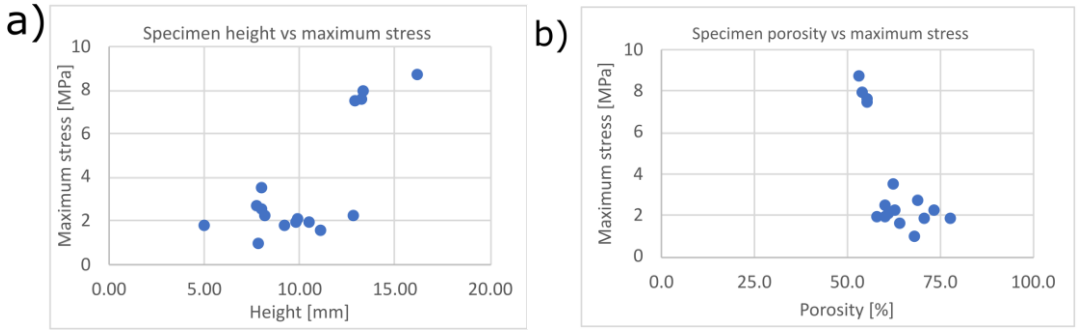

Figure 20. The scatter plot comparing the compressive strength of the samples against their heights (a) and against their porosity (b)

m [g]	D [mm]	H [mm]	Porosity [%]	Stress [MPa]
6.21	12.07	16.18	53.0	8.74
4.70	12.08	12.92	55.5	7.50
2.35	12.41	9.24	70.5	1.84
3.18	11.95	11.12	64.3	1.60
3.32	11.98	9.82	58.0	1.97
1.80	12.14	8.19	73.4	2.27
0.90	12.04	4.97	77.7	1.84
1.95	12.04	7.70	68.8	2.72
4.92	12.15	13.27	55.2	7.64
4.83	11.88	13.31	54.1	7.96
3.79	11.92	12.77	62.7	2.28
2.44	12.01	8.02	62.3	3.51
2.69	12.24	8.00	59.9	2.52
3.34	11.95	10.46	60.1	1.99
3.22	12.18	9.92	60.9	2.08
2.00	11.98	7.82	68.2	0.97

Table 1. all of the data of the samples from plotted in *Figure 20*a/b

Although these samples were produced with slight variations in production parameters (as discussed in the previous section), except the compacting time those parameters only affected the success in leaching and increased production efficiency, effects on strength were insignificant.

4.2 SEM and electron spectroscopy analysis

The first few specimens were investigated under an SEM to investigate the feasibility of chemical sintering. The results showed the successful formation of sintering necks visible on Figure 21a/b.

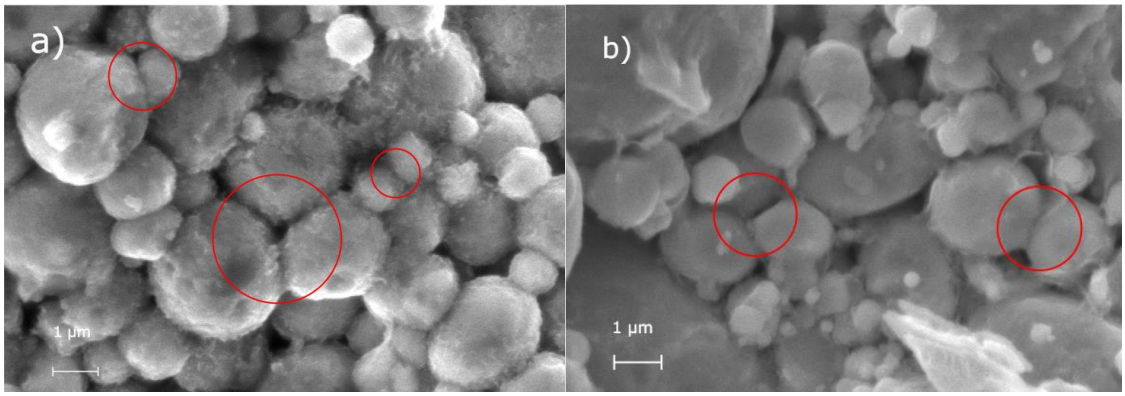

Figure 21 SEM images of one of the initial samples taken at different location with marked sintering necks shown on the left (a) and right (b) respectively

The problems with more recent specimens warranted a SEM investigation to check the formation of the sintering necks and an Z-ray micro-analysis (energy dispersive spectroscopy (EDS)) to find the cause of the low strength. The presence of new, differently looking particles could be clearly observed, as seen on Figure 22a/b.

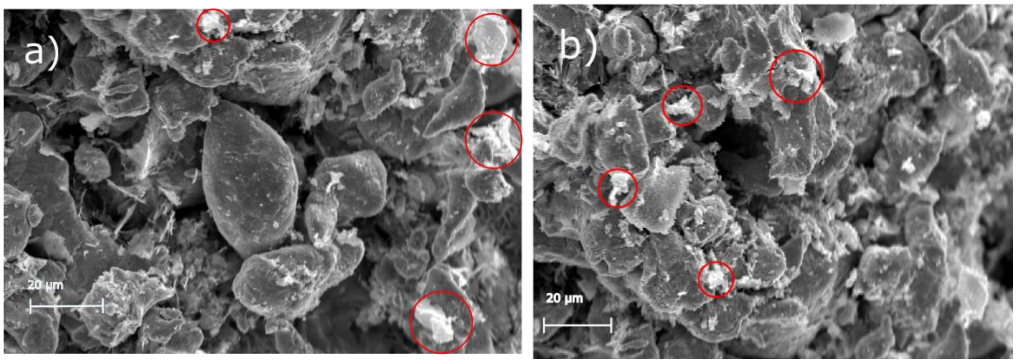

Figure 22. SEM images of the samples that were both chemically sintered and hot sintered for 1h (a) and 30 min (b) respectively

Using EDS, these bright structures were analysed and we found that the atomic oxygen content in these parts was much higher than in other regions, which signifies that these areas contain a higher amount of zinc oxide. The results of the spectroscopy can be seen on Figure 23a/b.

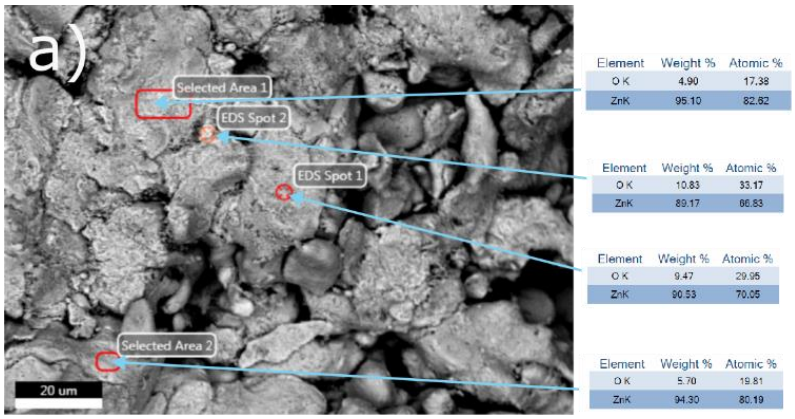

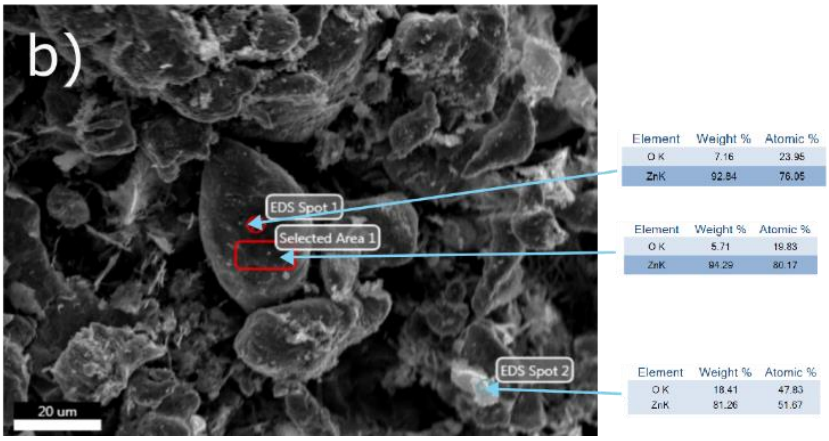

Figure 23. EDS results of the purely hot sintered sample (a) and the chemically sintered sample that was hot sintered for 30 min (b) respectively

It was concluded that the increased presence of zinc-oxide was the main reason for the decrease in strength of the specimens at the later stage of our research. This hypothesis is supported by the fact that the mechanical properties of the specimens became progressively worse even with improved manufacturing parameters and technique, which explains the low strength of the most recent hot sintered samples shown in Figure 19a/b/c.

5. Discussion

The initial research showed potential for a new technology of foam production, with clear sintering necks and noticeable mechanical strength. Further research managed to increase the consistency of sample production with improved production parameters. We found that the compaction time had the greatest effect on the mechanical properties, with an emphasis on the improved plateau region. More detailed investigations of this factor, as well as the potential of reducing hot sintering time were obstructed by the progressively increasing oxidation of the material used. This puts our conclusions that certain parameters didn't have an effect on the mechanical properties, such as compacting times shorter than 2h, into question as they might have been significantly affected by oxidization of the zinc powder. Although this does warrant the reinvestigation of some of the previous parameters it does not invalidate any of the positive effects observed with the variation of parameters, namely the compaction time.

According to our research, the most optimal specimens can be made with a 50:50 wt.% Zn:urea ratio using no more than 6 drops a 25:75 vol.% PVA: acetic acid solution as an adhesive. Most optimal mixing can be achieved by stirring it by any means in a container of similar dimensions to the final specimen. The mixture should be added in 3 increments into the die and no more than 2 drops of acid are recommended for each increment. The compacting pressure should be increased ideally up to 700MPa, but no less than 300MPa for sufficient sintering to occur. For a better plateau region compacting times of up to 2 hours are recommended. The samples should be left to dry for at least 24h before being grinded and leached in running water for 24 more hours. The exact effects of compacting times below 2 hours as well as the true maximum strength achieved by long compacting times could not be properly investigated due the zinc oxide layer hindering the neck formation during chemical and hot sintering.

6. Outlook

A lot of progress has been made with research of chemical sintering, especially in increasing the production efficiency and success rate. Although it was found that longer compaction times had the most significant effect on the mechanical properties, due to the interference of the zinc oxide the true effect of the other parameters might be more significant than what was observed. The future plans are to reinvestigate previous production parameters with non-oxidized zinc powder to test their true effect. An emphasis will be placed on the compaction times between 5 min and 2 hours because it was observed that compaction time had the biggest effect on the mechanical properties of the samples.

Acknowledgements

I would like to express my heartfelt thanks to the following people participated in this project and helped me with my struggles:

To Professor Thalmaier, for introducing me to the world of powder metallurgy as well as his bright ideas and innovative suggestions.

To my consultant, Dr. Wiener Csilla, for her guidance throughout the project, her unending support and patience as well as the knowledge she imparted to me.

In addition, I would like to express my thanks to the entirety of the Department of Material Science and Technology for the equipment provided for our research as well as all the colleagues for their occasional help.

References

1. *Commercial Applications of Metal Foams: Their Properties and Production.* **García-Moreno, F.** 2, 2016, Materials, Vol. 9, p. 85.

2. *Manufacture, characterisation and application of cellular metals and metal foams.* **Banhart, John.** 2001, Progress in Materials Science, pp. 559-632.

3. **China BeiHai.** Products. *Metal Foam Web.* [Online] 4 11 2023. https://www.metalfoamweb.com/aluminum-foam/closed-cell-aluminum-foam/.

4. *Computational reconstruction of scanned aluminum foams for virtual testing.* **Borovinšek, Matej & Vesenjak, Matej & Jože, M & Ren, Zoran.** 2008.

5. *Open Cell Metal Foams – Application-oriented Structure and Material Selection.* **P. Quadbeck, K. Kümmel, R. Hauser, G. Standke, J. Adler, G. Stephani.**

6. *Novel Lightweight Metal Foam Heat Exchangers.* **Haack, David P., Kenneth R. Butcher, T. Kim and Tian Jian Lu.** 2001, Process Industries.

7. *Heat transfer in open-cell metal foams.* **T.J. Lu, H.A. Stone, M.F. Ashby.** 1998, Acta Materialia, pp. 3619-3635.

8. *Crushing analysis of foam-filled single and bitubal polygonal thin-walled tubes.* **Zheng, Gang & Wu, Suzhen & Sun, Guangyong & Li, Guangyao & Li, Qing.** 2014, International Journal of Mechanical Sciences, Vol. 87, pp. 226-240.

9. *Mechanical behaviour and energy absorption of closed-cell aluminium foam panels in uniaxial compression.* **M.I. Idris, T. Vodenitcharova, M. Hoffman.** 1-2, 2009, Materials Science and Engineering: A, Vol. 517, pp. 37-45.

10. **Ashby, Anthony G. Evans and Michael F.** *Metal Foams: A Design Guide.* 2000. 9780080511467.

11. *Deformation characteristics of metal foams.* **J. BANHART, J. BAUMEISTER.** s.l. : Chapman & Hall, 1998.

12. *Properties of heat-treated aluminium foams.* **Dirk Lehmhus, John Banhart.** 1-2, 2003, Materials Science and Engineering: A, Vol. 349, pp. 98-110.

13. *Thermal Transport Phenomena in Porvair Metal Foams and Sintered Beds.* **Zhao, Chong & Kim, T & Lu, Tian & Hodson, Howard.** 2023.

14. **Rousell Goodall, A. Mortensen.** *Physical metallurgy.* 2014. pp. 2399-2595.

15. *Metal Foams: Fundamentals and Applications.* **Dukhan, Nihad, [ed.].** 2013.

16. *Foam stability in gas injection foaming process.* **Liu, X.N., Li, Y.X., Chen, X. et al.** 2010, J Mater Sci, Vol. 45, pp. 6481–6493.

17. *Selection of blowing agent for metal foam production: A review.* **A. Bisht, B. Gangil, V. K. Patel.** 1, 2020, J Met Mater Miner, Vol. 30.

18. *Powder metallurgy route aluminium foams: a study of the effect of powder morphology, compaction pressure and foaming temperature on the porous structure.* **I.G. Papantoniou, D.I. Pantelis, D.E. Manolakos.** 2018, Procedia Structural Integrity, pp. 243-248.

19. *Influence of processing parameters on aluminium foam produced by space holder technique.* **R. Surace, L.A.C. De Filippis, A.D. Ludovico, G. Boghetich.** 2009, Materials & Design, pp. 1878-1885.

20. *Mesostructural Design and Manufacturing of Open-Pore Metal Foams by Investment Casting.* **Alexander Martin Matz, Bettina Stefanie Mocker et al.** 2014.

21. *Implant biomaterials: A comprehensive review.* **Saini M, Singh Y, Arora P, Arora V, Jain K.** 2015, World J Clin Cases.

22. *Biodegradable bone implants in orthopedic applications: a review.* **Girish Chandra, Ajay Pandey.** 2, 2020, Biocybernetics and Biomedical Engineering, Vol. 40. 0208-5216.

23. *Biodegradable Materials and Metallic Implants-A Review.* **Prakasam M, Locs J, Salma-Ancane K, Loca D, Largeteau A, Berzina-Cimdina L.** 2017, J Funct Biomater.

24. *Production of high porosity Zn foams by powder metallurgy method.* **S. Sadighikia, S. Abdolhosseinzadeh & H. Asgharzadeh.** 1, Powder Metallurgy, Vol. 58, pp. 61-66.

25. *Comparison of zinc and aluminium foam behaviour .* **KOVACIK, J., SIMANCIK, F.** 2004, Metallic materials, pp. 79-90.

26. *Low temperature chemical sintering of inkjet-printed Zn nanoparticles for highly conductive flexible electronic components.* **Majee, S., Karlsson, M.C.F., Wojcik, P.J. et al.** 14, s.l. : Nature, 2021, Vol. 5.

27. *Cellular solids.* **Gibson, L.J.** s.l. : Springer Link, 2003.

28. *ISO 13314:2011.*

29. *Homogeneous Deposition of Zinc on Three-Dimensional Porous Copper Foam as a Superior Zinc Metal Anode.* Xiaodong Shi, Guofu Xu, Shuquan Liang, Canpeng Li, Shan Guo, Xuesong Xie, Xuemei Ma and Jiang Zhou. 2019, ACS Sustainable Chemistry & Engineering, pp. 17554-18196.

30. *Investigation of metal foam formation by microscopy and ultra small-angle neutron scattering.* J. Banhart, D. Bellmann, H. Clemens. 17, s.l. : Elsevier, 2001, Vol. 49. 1359-6454.

31. *Catalytic Metal Foam by Chemical Melting and Sintering of Liquid Metal Nanoparticles.* Allioux, F.-M., Merhebi, S., Tang, J., Idrus-Saidi, S. A., Abbasi, R., Saborio, M. G., Ghasemian, M. B., Han, J., Namivandi-Zangeneh, R., O'Mullane, A. P., Koshy, P., Daiyan, R., Amal, R., Boyer, C., Kalantar-Zadeh, K. s.l. : Wiley, 2020, Vol. 30. 1907879.

32. *Multifunctionality of cellular metal systems.* A.G. Evans, J.W. Hutchinson, M.F. Ashby. 1998, Progress in Materials Science, pp. 171-221.

33. ***Behavior of Metallic Foam under Shock Wave Loading.*** **Vesenjak, M., et al. 2012, Metals, pp. 258-264.**

34. BeiHai Composite. Featured. ***BeiHai Composites.*** **[Online] 4 11 2023. https://www.beihaicomposite.com/2021-high-quality-aluminium-foam-in-construction-composite-panel-beihai-product/.**

35. Interesting Engineering. Innovation. ***Interesting Engineering.*** **[Online] 4 11 2023. https://interestingengineering.com/innovation/inspired-by-nature-but-as-tough-as-iron-what-is-metal-foam-used-for.**

36. ***Low temperature chemical sintering of inkjet-printed Zn nanoparticles for highly conductive flexible electronic components.*** **Subimal Majee, Mikael C. F. Karlsson, Pawel Jerzy Wojcik, Anurak Sawatdee, Mohammad Yusuf Mulla, Naveed ul Hassan Alvi, Peter Dyreklev, Valerio Beni & David Nilsson. 2021, npj Flex Electronics.**